

Rotor in a Cage: Infrared Spectroscopy of an Endohedral Hydrogen-Fullerene Complex

S. Mamone,¹ Min Ge,² D. Hüvonen,² U. Nagel,² A. Danquigny,¹ F. Cuda,¹ M. C. Gossel,¹ Y. Murata,³ K. Komatsu,³ M. H. Levitt,¹ T. Rõõm,² and M. Carravetta^{1,*}

¹*School of Chemistry, Southampton University, Southampton SO17 1BJ, United Kingdom*

²*National Institute of Chemical Physics and Biophysics, Akadeemia tee 23, 12618 Tallinn, Estonia*

³*Institute for Chemical Research, Kyoto University, Kyoto 611-0011, Japan*

(Dated: October 29, 2018)

We report the observation of quantized translational and rotational motion of molecular hydrogen inside the cages of C₆₀. Narrow infrared absorption lines at the temperature of 6 K correspond to vibrational excitations in combination with translational and rotational excitations and show well-resolved splittings due to the coupling between translational and rotational modes of the endohedral H₂ molecule. A theoretical model shows that H₂ inside C₆₀ is a three-dimensional quantum rotor moving in a nearly spherical potential. The theory provides both the frequencies and the intensities of the observed infrared transitions. Good agreement with the experimental results is obtained by fitting a small number of empirical parameters to describe the confining potential, as well as the *ortho* to *para* ratio.

PACS numbers:

Endohedral complexes of H₂ molecules trapped inside fullerene cages have been synthesized recently[1, 2, 3]. Apart from their chemical interest and importance, these remarkable systems are ideal testbeds for the study of diatomic quantum rotors in a confined environment. H₂@C₆₀ is different from quantum rotors studied so far, which were two-dimensional or showed hindered rotation, like H₂ on a Cu surface[4], H₂ in intercalated graphite[5] or C₂ in a metallofullerene[6]. The small mass and large rotational constant of H₂ makes it the least sensitive of molecules to the corrugations of the potential surface. Also, C₆₀ provides a nearly spherical bounding potential. Theoretically it has been shown that in C₆₀ cages the quantum rotors CO[7] and H₂[8, 9] should have a measurable translation-rotation coupling, a feature that has not been experimentally resolved to our knowledge. Moreover, there is very little experimental information on the quantum dynamics of H₂ in fullerene cages[10, 11, 12, 13].

In general, isolated homonuclear diatomics have no infrared (IR) activity[14]. However, H₂ does display IR activity in situations where there are intermolecular interactions present, such as in the solid and liquid phases [15, 16], in constrained environments[17, 18, 19, 20], and in pressurized gasses[21, 22]. IR spectra of such systems are usually broad due to inhomogeneities in the system or due to random molecular collisions. As an exception, narrow lines are observed in semiconductor crystals[23] and solid hydrogen[24]. Similarly we expect narrow lines in solid H₂@C₆₀, where the broadening of IR lines is suppressed by homogeneous distribution of trapping potentials provided by C₆₀ molecules and by weak van der Waals interactions between the molecules.

In this Letter we study the dynamics of H₂ in cages of C₆₀ in the solid state with infrared spectroscopy. The observed spectra are described by a three-dimensional

quantum rotor confined in a nearly spherical potential exhibiting translation-rotation coupling.

The H₂@C₆₀ powder sample (10 mg) was prepared as described in [3] and pressed into a $d = 0.25$ mm thick pellet. IR transmission measurements were made with an interferometer Vertex 80v (Bruker), halogen lamp, and MCT detector with an apodized resolution 0.3 cm^{-1} . The sample and the reference open hole were inside an optical cryostat with KBr windows. The absorption coefficient $\alpha(\omega)$ was calculated from the transmission $T_r(\omega)$ through $\alpha(\omega) = -d^{-1} \ln [T_r(\omega)(1 - R)^{-2}]$ with the reflection coefficient $R = [(n - 1)/(n + 1)]^2$. A frequency-independent index of refraction $n = 2$ was assumed [25]. The low temperature IR absorption peaks of H₂@C₆₀ are located in four narrow spectral bands between 4060 and 4810 cm^{-1} , see Fig.1. This region corresponds to the H₂ stretching mode and its rotational/translational sidebands. Peaks in 4250 cm^{-1} , 4600 cm^{-1} and 4800 cm^{-1} regions (panels b, c, and d in Fig.1) are assigned to vibrational excitations of H₂ accompanied by translational and/or rotational excitations. It is the translation-rotation coupling that splits the $Q(1)$ line, shown in Fig.1b, into three peaks. Weak transitions around 4070 cm^{-1} (Fig.1a) represent pure vibrational excitations of the H₂ molecule and are forbidden in the approximate theory presented below.

The position and orientation of the H₂ molecule is described using spherical coordinates $\mathbf{R} = \{R, \Theta, \Phi\}$ and $\mathbf{r} = \{r, \theta, \phi\}$ where \mathbf{R} is the vector from the center of the C₆₀ cage to the center of mass of H₂ and \mathbf{r} is the internuclear H-H vector. As first approximation we consider decoupled translational, rotational and vibrational movement of H₂. The translation of the confined molecule may be treated using the isotropic three-dimensional harmonic oscillator model. The appropriate translational

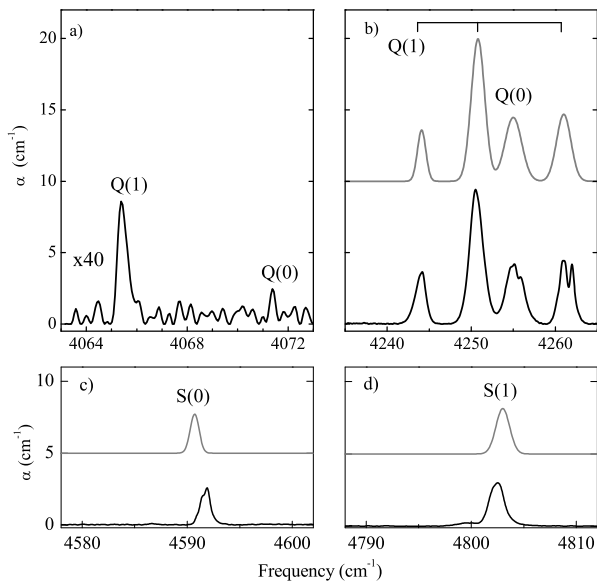


FIG. 1: Baseline-corrected IR absorption spectra of $\text{H}_2@C_{60}$ at 6 K (black) and the best fit theoretical spectrum (grey) in panels (b), (c), and (d). All transitions are from the vibrational state $v = 0$ to $v = 1$. The letter indicates the change in J (Q for $\Delta J = 0$ and S for $\Delta J = 2$) and the number in parentheses is the initial J value. For the assignment inside a rotational branch, see Table I and Fig. 2. (a) Fundamental vibrational transitions; these are forbidden in the first-order theory so a simulated spectrum is not shown. (b) $\Delta J = 0$, $\Delta N = +1$ transitions. (c) *para*- H_2 and (d) *ortho*- H_2 S transitions with $\Delta N = +1$, $\Delta J = +2$.

quantum numbers are $N = 0, 1, \dots$, the orbital angular momentum quantum number L , which is an integer with the same parity as N and the azimuthal quantum number M_L . The radial part of the wavefunction depends both on N and L . The translational eigenfunctions are $\Psi_{NLM_L}^T(R, \Theta, \Phi) = \Psi_{NL}^T(R)Y_{LM_L}(\Theta, \Phi)$ where the radial wave function Ψ_{NL}^T and the spherical harmonics Y_{LM_L} are defined in [26]. The rotational wavefunctions, defined by the rotational quantum numbers $J = 0, 1, \dots$ and $M_J = -J, -J + 1, \dots, +J$, are given by the spherical harmonics $Y_{JM_J}(\theta, \phi)$. It is convenient to use bipolar spherical harmonics with overall spherical rank Λ and component M_Λ , defined as follows:

$$F_{\Lambda M_\Lambda}^{LJ}(\Omega) = \sum_{M_L, M_J} C_{LM_L J M_J}^{\Lambda M_\Lambda} Y_{LM_L}(\Theta, \Phi) Y_{JM_J}(\theta, \phi), \quad (1)$$

where $\Omega = \{\Theta, \Phi, \theta, \phi\}$ and C are the Clebsch-Gordan coefficients [27]. The full wavefunction describing the motion of the H_2 molecule may be written as $|vJNL\Lambda M_\Lambda\rangle = \Psi_v^V(r)\Psi_{NL}^T(R)F_{\Lambda M_\Lambda}^{LJ}(\Omega)$ where $\Psi_v^V(r)$ is the vibrational wavefunction with a quantum number v . The total nuclear spin I of the H_2 molecule determines whether it is either in a *para* state ($I = 0$ and J even) or in an *ortho* state ($I = 1$ and J odd). The Hamiltonian \mathcal{H} for the trapped molecule includes coupling terms between the vi-

brational, translational, and rotational motion. For simplicity, we neglect all matrix elements non-diagonal in v and introduce a parametric dependence on v :

$$\mathcal{H} = {}^v\mathcal{H}^{VR} + \frac{p^2}{2m} + {}^vV(R, \Omega), \quad (2)$$

where ${}^v\mathcal{H}^{VR}$ is the vibration-rotation Hamiltonian, p is the molecular momentum operator and m is the molecular mass. The superscript prefix v is used to indicate an implied dependence on the vibrational quantum number. vV is the potential energy of a molecule at a given position and orientation within the cavity, and includes terms that couple the rotational and translational motion. The vibrational-rotational Hamiltonian ${}^v\mathcal{H}^{VR}$ is diagonal in the basis set $|vJNL\Lambda M_\Lambda\rangle$ with eigenvalues given by ${}^vE_J^{VR} = \hbar\omega_0^V(v + 1/2) + B_v J(J + 1)$, where ω_0^V is the fundamental vibration frequency; $B_v = B_e - \alpha_e(v + 1/2)$, where α_e is an anharmonic correction to the rotational constant B_e [14]. Below 120 K, the thermally-activated rotational motion of the C_{60} cages is suppressed [13, 28] and vV may be assumed to be time-independent. Expanded in multipoles it reads:

$${}^vV(R, \Omega) = \sum_{n,l,j,\lambda,m_\lambda} {}^vV_{\lambda m_\lambda}^{ljn} R^n F_{\lambda m_\lambda}^{lj}(\Omega), \quad (3)$$

where the functions F are defined in Eq. 1 and n takes even values. Terms with $n = 2$ constitute a harmonic potential energy function, while terms with $n > 2$ represent anharmonic perturbations. Translation-rotation coupling terms are terms with non-zero l, j .

All odd- j terms vanish for homonuclear diatomic molecules. For an icosahedral cavity, and assuming that longer-range intermolecular perturbations are negligible, all terms with odd λ values vanish, as well as the terms with $\lambda = 2$ and 4. We assume that all high-order terms starting from $\lambda = 6$ are small and express the potential energy as ${}^vV = {}^vV^0 + {}^vV'$, where the isotropic harmonic term is given by ${}^vV^0 = {}^vV_{00}^{000} F_{00}^{00} + {}^vV_{00}^{002} R^2 F_{00}^{00}$ and the perturbation due to translation-rotation and anharmonic coupling is given by ${}^vV' \cong {}^vV_{00}^{222} R^2 F_{00}^{22} + {}^vV_{00}^{004} R^4 F_{00}^{00}$. The unperturbed Hamiltonian eigenvalues in the basis $|vJNL\Lambda M_\Lambda\rangle$ are given by $E_{vJNL\Lambda M_\Lambda}^0 = {}^vE_J^{VR} + \hbar v \omega_0^T(N + 1/2)$, where $\omega_0^T = ({}^vV_{00}^{002}/(2\pi m))^{1/2}$ is the frequency for translational oscillations within the cavity.

The matrix elements of ${}^vV'$ were evaluated analytically in the basis $|vJNL\Lambda M_\Lambda\rangle$ using 100 states with $N \leq 2$ and $J = 1, 3$ for *ortho*- H_2 , and 60 states with $N \leq 2$ and $J = 0, 2$ for *para*- H_2 . Matrix diagonalization leads to explicit but cumbersome expressions for the energy levels and eigenstates. A schematic energy level diagram is given in Fig. 2. The ordering of the eigenvalues depends on the relative sign and magnitudes of the anharmonic term ${}^vV_{00}^{004}$ and the translation-rotation coupling term ${}^vV_{00}^{222}$. The ordering in Fig. 2 is consistent with the experimental results.

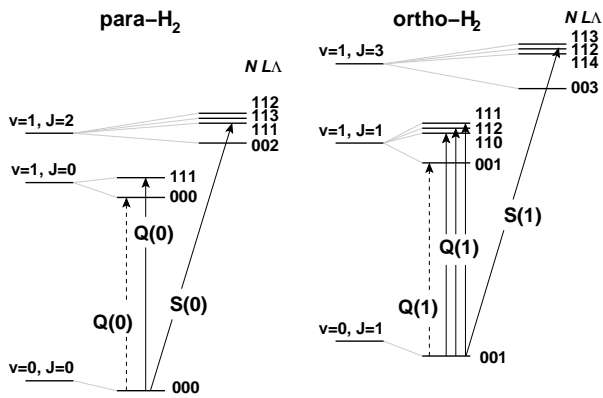


FIG. 2: Diagram of H₂ energy levels refined against low-*T* IR data. For the $v = 0$ state only the ground state rotational and translational levels are shown. The energy levels of free H₂ are shown on the left while the effect of confinement by C₆₀ is shown on the right, both for *para*- and *ortho*-H₂. The arrows show transitions corresponding to the observed low-*T* IR peaks. The transitions marked by dashed lines are forbidden within the theory presented here.

IR activity in H₂@C₆₀ is due to a dipole moment, μ , induced by the constraining environment. The dipole moment operator can be expanded in multipoles depending on the instantaneous H₂ configuration [29]:

$$\mu_q = \frac{4\pi}{\sqrt{3}} \sum_{l,j=0}^{\infty} A^{lj}(R, r) F_{1q}^{lj}(\Omega), \quad (4)$$

where q denotes the spherical component and the A coefficients describe the induced dipole moment. Since the dipole moment is a vector, there are restrictions on the allowed j and l values: (i) $j + l$ must be odd, (ii) $l = j \pm 1$ from the triangle relation, (iii) for homonuclear molecules only even j terms are allowed. These restrictions imply selection rules for IR spectroscopy of H₂@C₆₀. The selection rule for the total angular momentum is $\Delta\Lambda = 0, \pm 1$ with the only allowed transitions having even values of ΔJ and odd values of ΔL . In addition, because only the ground translational states ($N = L = 0$) are populated at low temperature, the allowed transitions observed in the 6 K IR spectrum are to $N = L = 1$ states (Fig. 2).

The IR absorption amplitude at frequency ω is [14]:

$$S_\omega \propto \omega \sum_{i,f} p_i(n_K, T) |\langle f | \mu_q | i \rangle|^2 \delta(E_f - E_i - \omega), \quad (5)$$

where $K = O$ or P selects *ortho*- or *para*-H₂. At the sample temperature T , the fractional population $p_i(n_K, T)$ of the initial state $|i\rangle$ is given by the Boltzmann distribution for *ortho* and *para* manifolds separately. Since the spin isomer interconversion is negligible for the endohedral complex [13], the number of *ortho* and *para* molecules, n_O and n_P , is not in general governed by the Boltzmann distribution and must be determined empirically. Since all the observed transitions are from $L = 0$ to $L = 1$, only

TABLE I: Experimental and calculated center frequencies, ω , and absorption line areas, S_ω , of IR-active H₂ modes at 6 K in H₂@C₆₀. The forbidden transitions (Fig. 1a and dotted lines in Fig. 2) are used as frequency references for the fitting procedure.

	NLA		Experimental		Fitted	
	initial	final	ω (cm ⁻¹)	S_ω (cm ⁻²)	ω (cm ⁻¹)	S_ω (cm ⁻²)
Q(1)	001	001	4065.44	0.093		
Q(0)	000	000	4071.39	0.011		
Q(1)	001	111	4244.5	5.6	4244.1	4.5
Q(1)	001	112	4250.7	18.8	4250.7	20.0
Q(1)	001	110	4261.0	8.7	4261.0	10.0
Q(0)	000	111	4255.0	10.5	4255.5	11.2
S(0)	000	111	4591.5	3.1	4590.7	2.9
S(1)	001	112	4802.5	5.6	4803.0	5.1

terms with $l = 1$ and $j = 0, 2$ are to be considered in the dipole expansion. This implies that only $\Delta J = 0, +2$ transitions are observable. The dipole matrix elements for the observed transitions in H₂@C₆₀ between states $|i\rangle$ and $|f\rangle$ can be expressed as

$$\langle f | \mu_q | i \rangle = \frac{4\pi}{\sqrt{3}} \sum_{j=0,2} \rho^j [X_{1q}^{1j}]_{fi}, \quad (6)$$

where $\rho^j = \langle \Psi_1^V(r) \Psi_{11}^T(R) | A^{1j}(R, r) | \Psi_0^V(r) \Psi_{00}^T(R) \rangle$ and $[X_{1q}^{1j}]_{fi} = \langle F_f(\Omega) | F_{1q}^{1j}(\Omega) | F_i(\Omega) \rangle$. The matrix elements reduce into a sum of products over radial integrals ρ^j and known angular integrals.

Three potential parameters ${}^1V_{00}^{002}$, ${}^1V_{00}^{222}$, ${}^1V_{00}^{004}$, the rotational constant B_e , and $\rho^0, \rho^2, n_O/n_P$ were fitted to match the experimental frequencies and intensities. The potential parameters in the first vibrational state are $\{{}^1V_{00}^{002}, {}^1V_{00}^{222}\} = \{27 \pm 6, 1.5 \pm 0.2\}$ J m⁻² and ${}^1V_{00}^{004} = (-2 \pm 20) 10^{20}$ J m⁻⁴. The low-*T* data is insufficient to derive accurately the anharmonic correction ${}^1V_{00}^{004}$, which is poorly defined from the separation of $N = 0$ and $N = 1$ levels only. This affects the value of ${}^1V_{00}^{002}$, because ${}^1V_{00}^{002}$ and ${}^1V_{00}^{004}$ are correlated. However, the translation-rotation coupling term ${}^1V_{00}^{222}$ is well-defined. ${}^1V_{00}^{222}$ and ${}^1V_{00}^{004}$ describe the potential within approximately 0.5 Å from the C₆₀ cage center, which is the root square of the average square displacement for the $N = 1$ translational state. The fitted rotational constant is $B_e = 59.3 \pm 0.2$ cm⁻¹ while $\alpha_e = 2.98 \pm 0.10$ cm⁻¹ is obtained directly from the difference in the fundamental vibrational frequencies for the *ortho*- and *para*-H₂. The ratio between the induced dipole moment parameters is $\rho^0/\rho^2 = -2.0 \pm 0.2$. The *ortho* to *para* ratio $n_O/n_P = 2.8 \pm 0.2$ is consistent with the equilibration at any temperature warmer than 120K and suggests that there has been negligible spin isomer interconversion since the molecules were synthesized. The data and the best fit results are displayed in Fig. 1 and summarized in Table I. The frequencies of the pure vibrational transitions (Fig. 1a) are shifted by -90 cm⁻¹ from the free H₂

value. The reduction in both the vibrational frequency and the rotational constant [30] are consistent with a predominantly attractive C-H interaction that slightly stretches the H-H bond.

The results described here are in qualitative agreement with previous theoretical studies. The quantum-chemical calculation by Cross[8] gave a factor of two smaller translation-rotation coupling potential term and larger values for both harmonic and anharmonic potential terms, leading to significant discrepancies in the IR line positions if used to reproduce the experimental data. Xu *et al.*[9] used pair-wise Lennard-Jones potentials in their quantum-mechanical calculation. The ordering of the Λ sublevels is consistent with our results, even though the splittings are different. Xu *et al.* used two different potential energy surfaces, which gave different $\nu\omega_0^T$, one smaller and the other larger than the experimentally observed $\nu\omega_0^T$. The splitting among the $J = N = 1$ energy levels, that is the measure of νV_{00}^{222} , remained larger than the experimentally observed value for both potential energy surfaces. Although our measurements refer to the $v = 1$ excited state, while the numerical calculations are for the $v = 0$ ground state, it seems that the theory using a pairwise C-H potential is not accurate enough to describe the dynamics of $\text{H}_2@C_{60}$. We believe that our results are a reference for theories modeling the interaction between H_2 and curved carbon nano-surfaces.

Deformation of the cage, crystal field, or carbon isotopomers in the cage may lower the symmetry and split the 4255 and 4261 cm^{-1} lines (Fig. 1b) and cause the IR activity of the weak fundamental transitions (Fig. 1a).

In summary, the IR spectrum of endohedral H_2 displays a rich structure due to the coupled translational and rotational modes of the confined quantum rotor. Line positions *and* intensities are described by a theory involving multipole expansion of the confining potential and fitting of a small number of parameters. The next targets will be analyzing higher- T data to extract information about anharmonic corrections and the vibrational ground state, studying lower symmetry cages and different dihydrogen isotopomers. The accurate determination of the energy levels in the vibrational ground state may play a key role in understanding fully the low- T NMR-behavior of endohedral H_2 in different fullerenes[13].

The support by the EPSRC, the EstSF grants 6138 and 7011, and the University Research Fellowship (Royal Society) is acknowledged. S.M. thanks Dr. G. Pileio for useful discussions.

* Electronic address: marina@soton.ac.uk

[1] Y. Rubin, T. Jarrosson, G.-W. Wang, M. D. Bartberger, K. N. Houk, G. Schick, M. Saunders, and R. J. Cross, *Angew. Chem. Int. Ed.* **40**, 1543 (2001).

- [2] K. Komatsu, M. Murata, and Y. Murata, *Science* **307**, 238 (2005).
- [3] M. Murata, Y. Murata, and K. Komatsu, *J. Am. Chem. Soc.* **128**, 8024 (2006).
- [4] A. P. Smith, R. Benedek, F. R. Trouw, M. Minkoff, and L. H. Yang, *Phys. Rev. B* **53**, 10187 (1996).
- [5] L. Bengtsson, K. Svensson, M. Hassel, J. Bellman, M. Persson, and S. Andersson, *Phys. Rev. B* **61**, 16921 (2000).
- [6] M. Krause, M. Hulman, H. Kuzmany, O. Dubay, G. Kresse, K. Vietze, G. Seifert, C. Wang, and H. Shinohara, *Phys. Rev. Lett.* **93**, 137403 (2004), URL <http://link.aps.org/abstract/PRL/v93/e137403>.
- [7] E. H. T. Olthof, A. van der Avoird, and P. E. S. Wormer, *J. Chem. Phys.* **104**, 832 (1996), URL <http://link.aip.org/link/?JCP/104/832/1>.
- [8] R. J. Cross, *J. Phys. Chem. A* **105**, 6943 (2001).
- [9] M. Xu, F. Sebastianelli, Z. Bačić, R. Lawler, and N. J. Turro, *J. Chem. Phys.* **129**, 064313 (2008), URL <http://link.aip.org/link/?JCP/129/064313/1>.
- [10] P. M. Rafailov, C. Thomsen, A. Bassil, K. Komatsu, and W. Bacsá, *Phys. Stat. Sol. (b)* **242**, R106 (2005).
- [11] E. Sartori, M. Ruzzi, N. J. Turro, J. D. Decatur, D. C. Doetschman, R. G. Lawler, A. L. Buchachenko, Y. Murata, and K. Komatsu, *J. Am. Chem. Soc.* **128**, 14752 (2006).
- [12] M. Carravetta, O. G. Johannessen, M. H. Levitt, I. Heinmaa, R. Stern, A. Samoson, A. J. Horsewill, Y. Murata, and K. Komatsu, *J. Chem. Phys.* **124**, 104507 (2006).
- [13] M. Carravetta, A. Danquigny, S. Mamone, F. Cuda, O. G. Johannessen, I. Heinmaa, K. Panesar, R. Stern, M. C. Grossel, A. J. Horsewill, et al., *Phys. Chem. Chem. Phys.* **9**, 4879 (2007).
- [14] G. Herzberg, *Molecular spectra and molecular structure, I. Spectra of diatomic molecules* (Van Nostrand Company, Inc. (Princeton), 1950), 2nd ed.
- [15] E. J. Allin, W. F. J. Hare, and R. E. MacDonald, *Phys. Rev.* **98**, 554 (1955).
- [16] W. F. J. Hare, E. J. Allin, and H. L. Welsh, *Phys. Rev.* **99**, 1887 (1955).
- [17] B. Hourahine and R. Jones, *Phys. Rev. B* **67**, 121205 (2003).
- [18] S. A. FitzGerald, S. Forth, and M. Rinkoski, *Phys. Rev. B* **65**, 140302 (2002).
- [19] S. A. FitzGerald, H. O. H. Churchill, P. M. Korngut, C. B. Simmons, and Y. E. Strangas, *Phys. Rev. B* **73**, 155409 (2006).
- [20] R. M. Herman and J. C. Lewis, *Phys. Rev. B* **73**, 155408 (2006).
- [21] A. Kudian and M. Welsh, *Can. J. Phys.* **49**, 230 (1971).
- [22] A. R. W. McKellar and H. L. Welsh, *Can. J. Phys.* **52**, 1082 (1974).
- [23] E. E. Chen, M. Stavola, W. B. Fowler, and P. Walters, *Phys. Rev. Lett.* **88**, 105507 (2002).
- [24] T. Oka, *Annu. Rev. Phys. Chem.* **44**, 299 (1993).
- [25] C. C. Homes, P. J. Horoyski, M. L. W. Thewalt, and B. P. Clayman, *Phys. Rev. B* **49**, 7052 (1994).
- [26] S. Flügge, *Practical quantum mechanics* (Springer-Verlag (Berlin), 1971).
- [27] D. A. Varshalovich, A. N. Moskalev, and V. K. Khersonskii, *Quantum Theory of Angular Momentum* (World Scientific, Singapore, 1988).
- [28] R. Tycko, G. Dabbagh, R. M. Fleming, R. C. Haddon, A. V. Makhija, and S. M. Zahurak, *Phys. Rev. Lett.* **67**,

1886 (1991).

[29] J. D. Poll and J. L. Hunt, *Can. J. Phys.* **54**, 461 (1976).

[30] S. Bragg, J. Brault, and W. Smith, *Astrophys. J.* **263**,

999 (1982).